

Supporting Information

High selectivity and significant cytotoxicity of rare earth naphthalene dicarboxylate complexes on non-small cell lung cancer cells

Hao Wang^c, Jiaxin Wang^b, Rui Wang^{a,*} and Liang Zhou^{a,*}

^a State Key Laboratory of Rare Earth Resource Utilization, Changchun Institute of

Applied Chemistry, Chinese Academy of Sciences, Changchun, 130022, China;

^b Jilin Medical Device Inspection and Research Institute, Changchun, 130062, China;

^c School of Materials Science and Engineering, Jilin Jianzhu University, Changchun

130118, China.

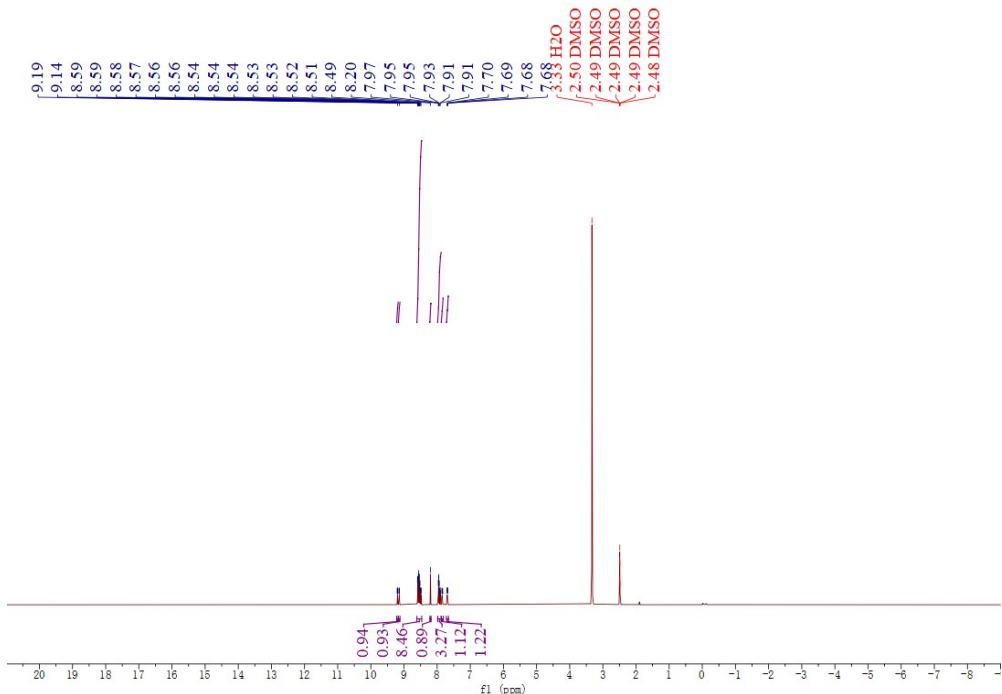


Figure S1. ^1H NMR spectrum of NI-Phen.

*Correspondence to: State Key Laboratory of Rare Earth Resource Utilization, Changchun Institute of Applied Chemistry, Chinese Academy of Sciences, Renmin Street 5625, Changchun 130022, China. Tel: +86 431 85262855; fax: +86 431 85698041.

*E-mail address: wangrui1123@ciac.ac.cn (R. Wang), and zhoul@ciac.ac.cn (L. Zhou).

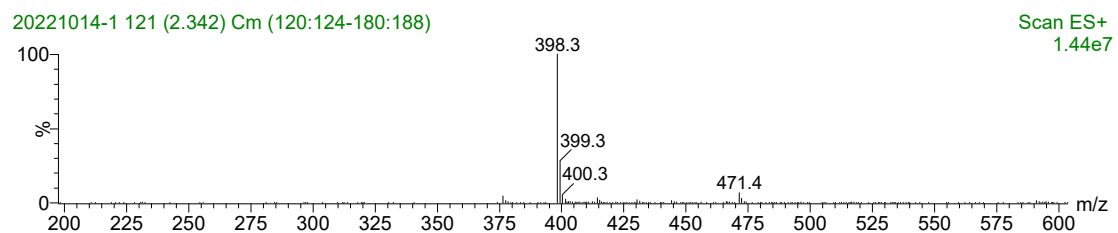


Figure S2. ESI-MS spectrum of Ni-Phen.

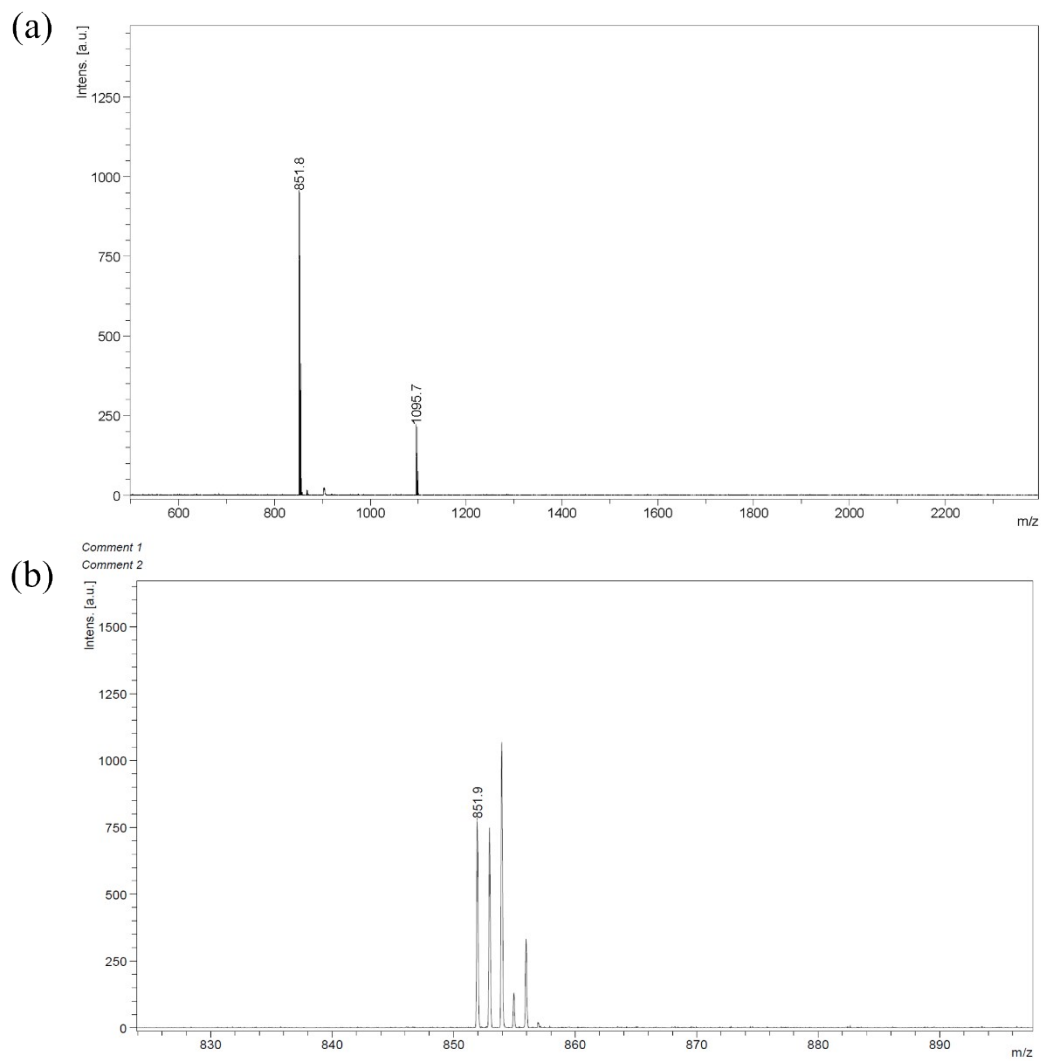


Figure S3. (a) MALDI-TOF-MS spectrum of $\text{Er}(\text{TTA})_3\text{H}_2\text{O}$. (b) Magnified MALDI-TOF-MS spectrum of $\text{Er}(\text{TTA})_3\text{H}_2\text{O}$.

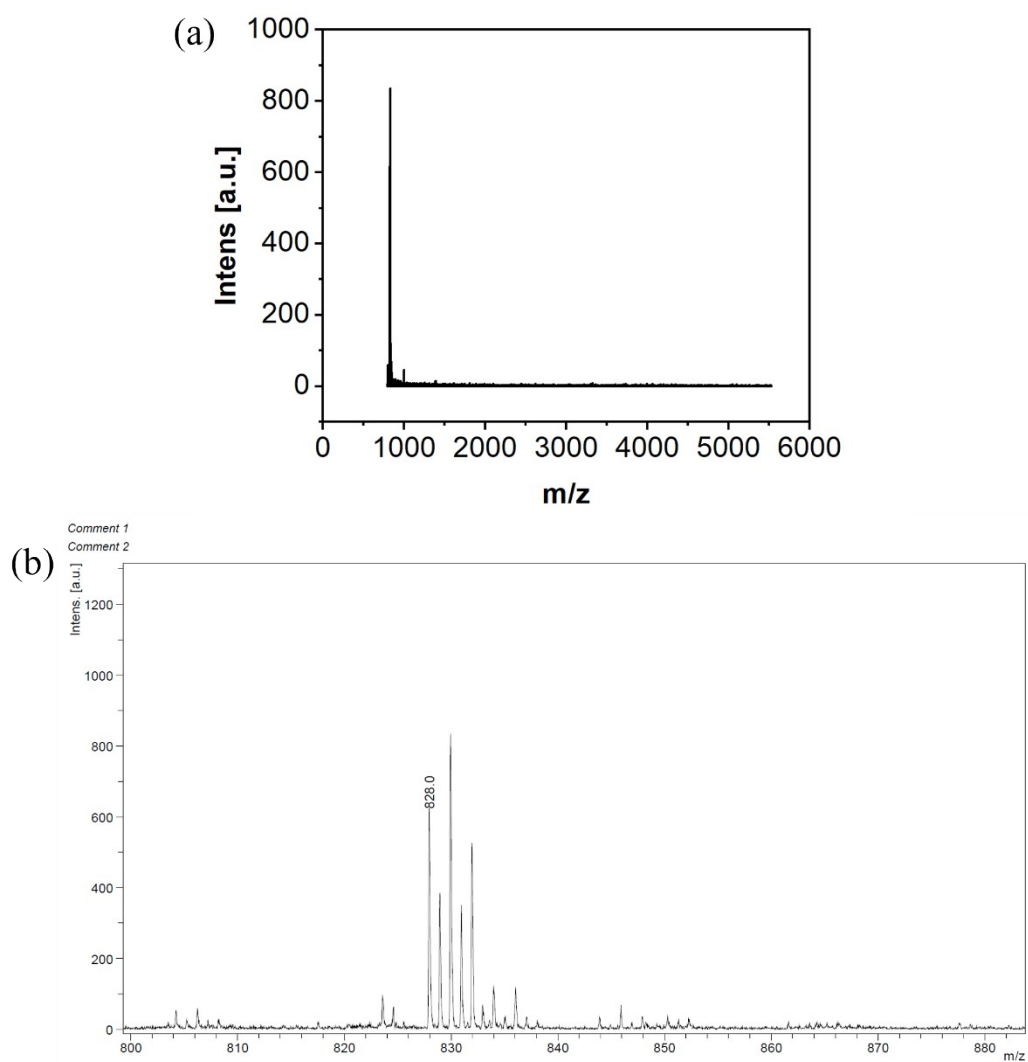


Figure S4. (a) MALDI-TOF-MS spectrum of $\text{Nd}(\text{TTA})_3 \cdot 2\text{H}_2\text{O}$. (b) Magnified MALDI-TOF-MS spectrum of $\text{Nd}(\text{TTA})_3 \cdot 2\text{H}_2\text{O}$.

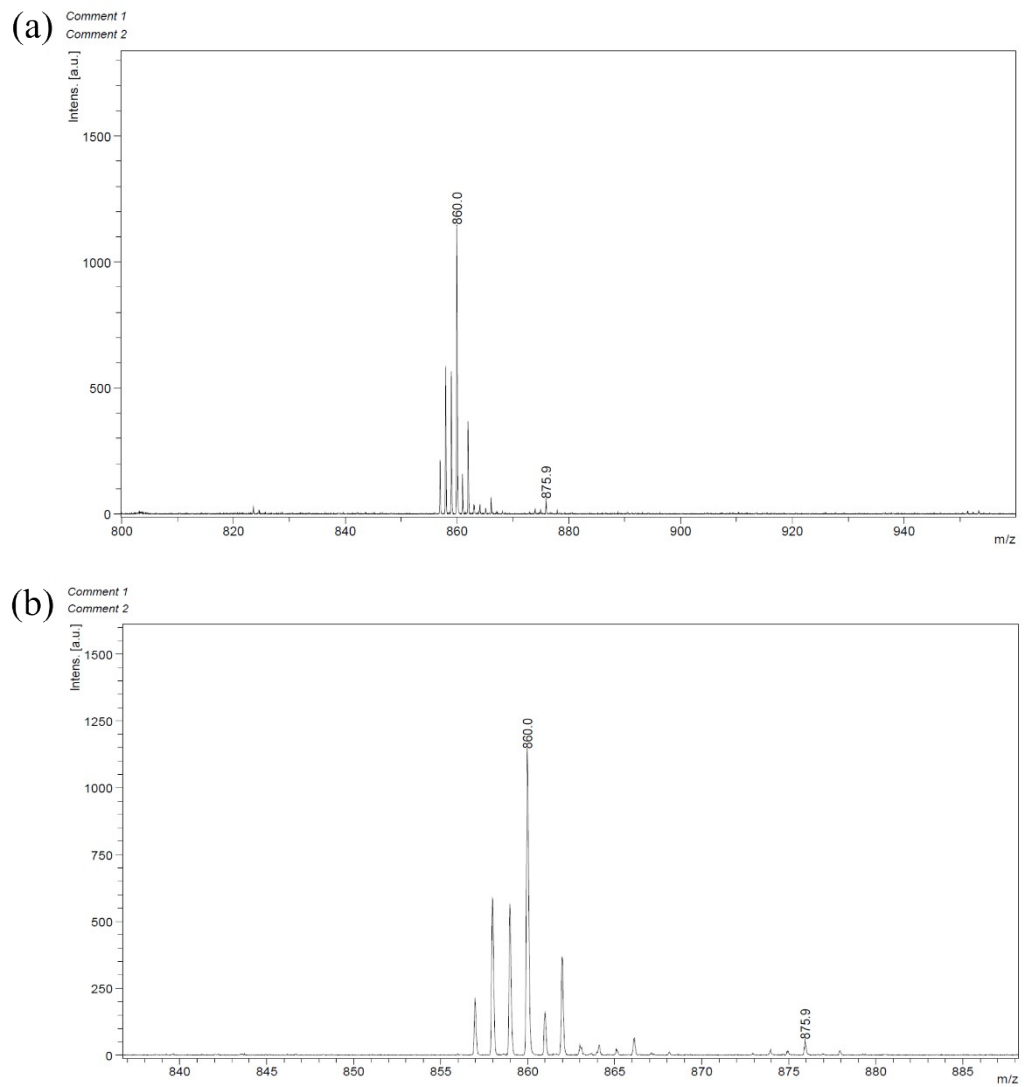


Figure S5. (a) MALDI-TOF-MS spectrum of $\text{Yb}(\text{TTA})_3 \cdot 2\text{H}_2\text{O}$. (b) Magnified MALDI-TOF-MS

spectrum of $\text{Yb}(\text{TTA})_3 \cdot 2\text{H}_2\text{O}$.

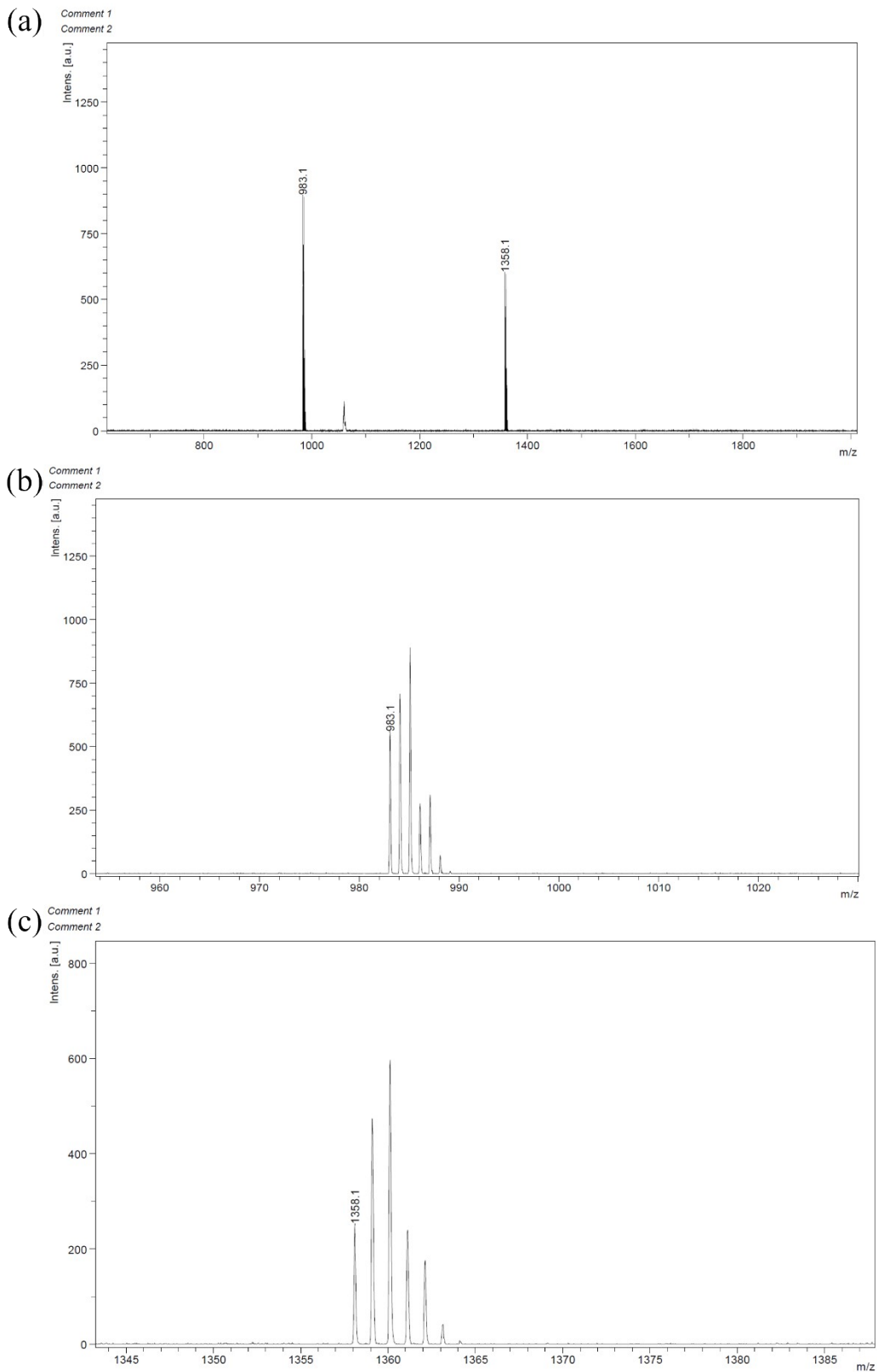


Figure S6. (a) MALDI-TOF-MS spectrum of $\text{Er}(\text{TTA})_3\text{Ni-Phen}$. (b, c) Magnified MALDI-TOF-MS spectrum of $\text{Er}(\text{TTA})_3\text{Ni-Phen}$.

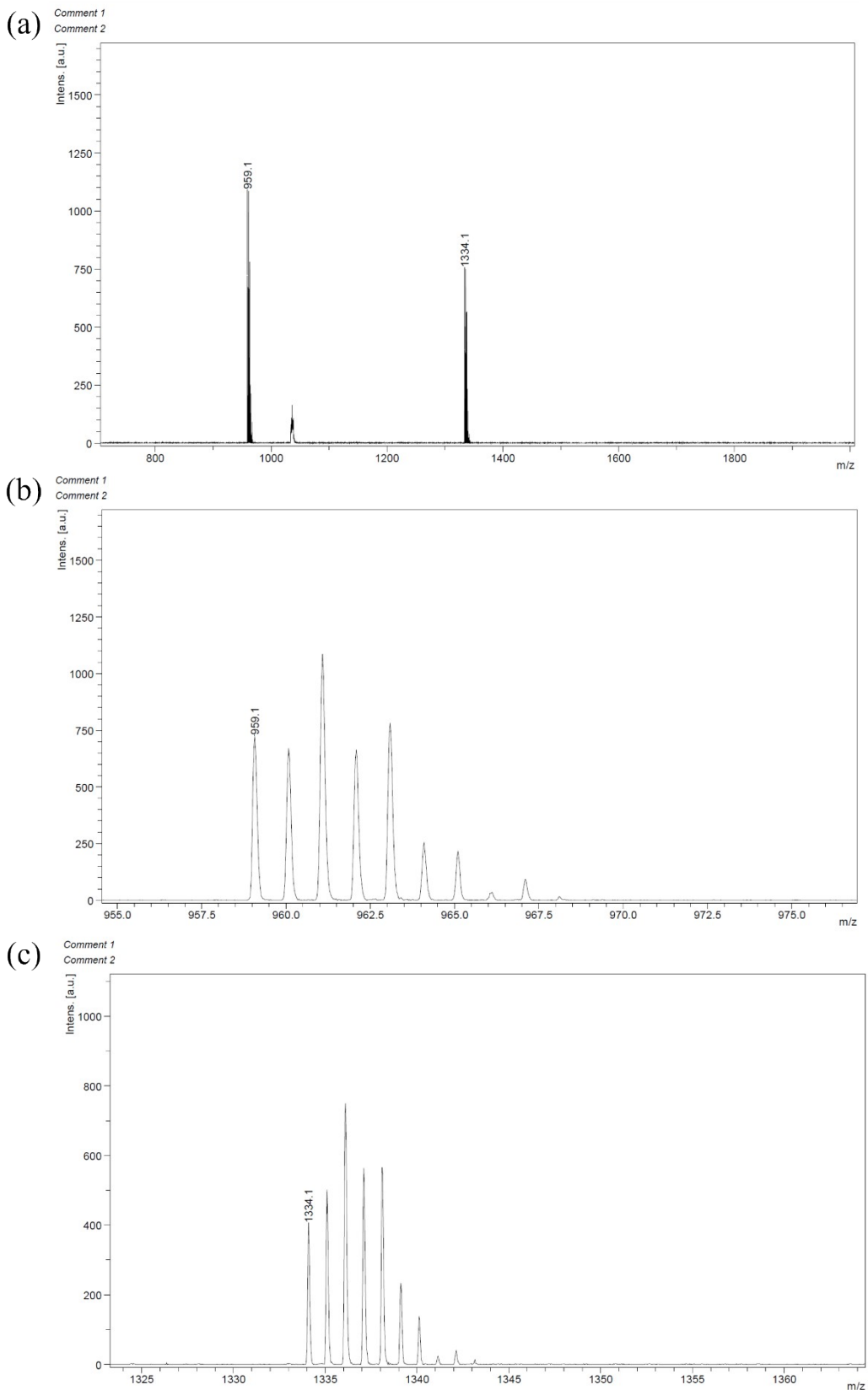


Figure S7. (a) MALDI-TOF-MS spectrum of Nd(TTA)₃Ni-Phen. (b, c) Magnified MALDI-TOF-MS spectrum of Nd(TTA)₃Ni-Phen.

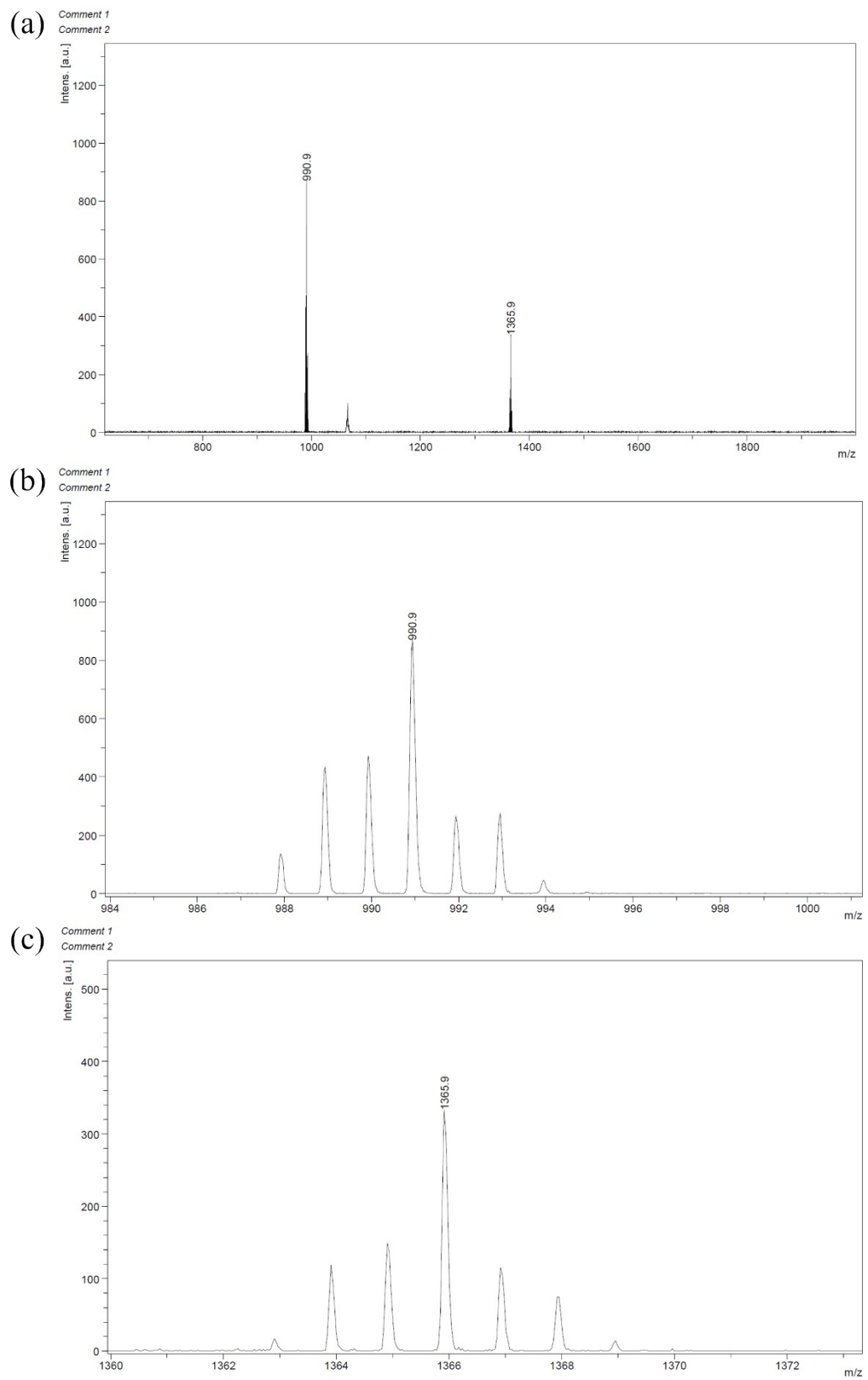


Figure S8. (a) MALDI-TOF-MS spectrum of $\text{Yb}(\text{TTA})_3\text{Ni-Phen}$. (b, c) Magnified MALDI-TOF-MS spectrum of $\text{Yb}(\text{TTA})_3\text{Ni-Phen}$.

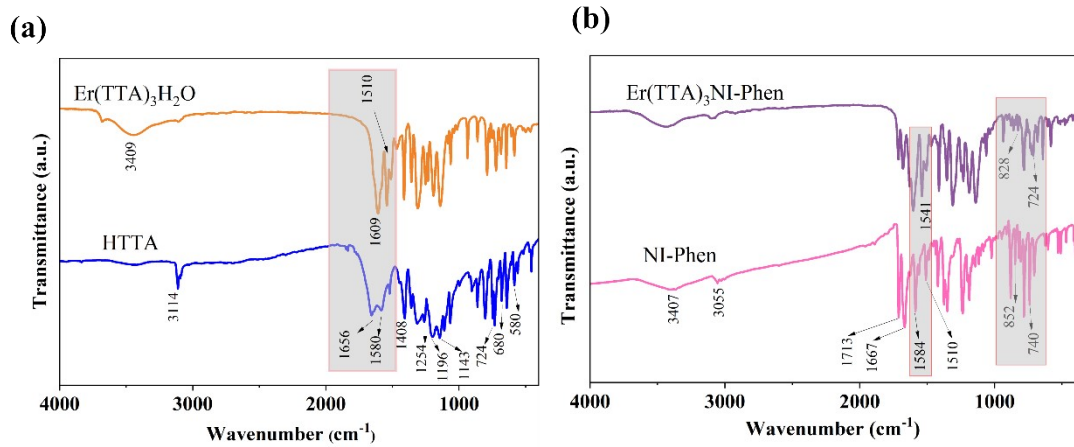


Figure S9. FT-IR spectra of (a): $\text{Er}(\text{TTA})_3\text{H}_2\text{O}$ and HTTA. (b): $\text{Er}(\text{TTA})_3\text{NI-Phen}$ and NI-Phen.

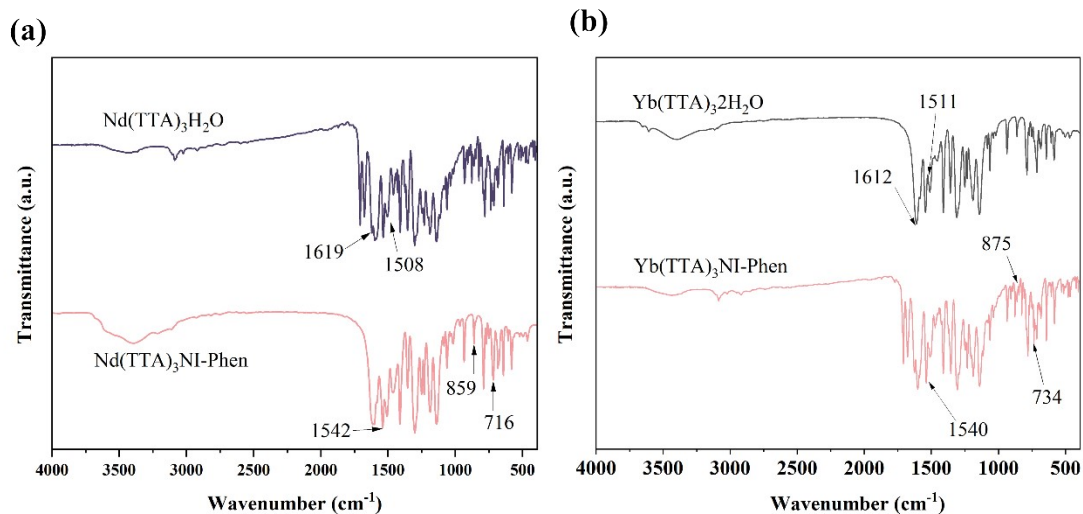


Figure S10. FT-IR spectra of (a): $\text{Nd}(\text{TTA})_32\text{H}_2\text{O}$ and $\text{Nd}(\text{TTA})_3\text{NI-Phen}$, (b): $\text{Yb}(\text{TTA})_32\text{H}_2\text{O}$ and $\text{Yb}(\text{TTA})_3\text{NI-Phen}$.

and $\text{Yb}(\text{TTA})_3\text{NI-Phen}$.

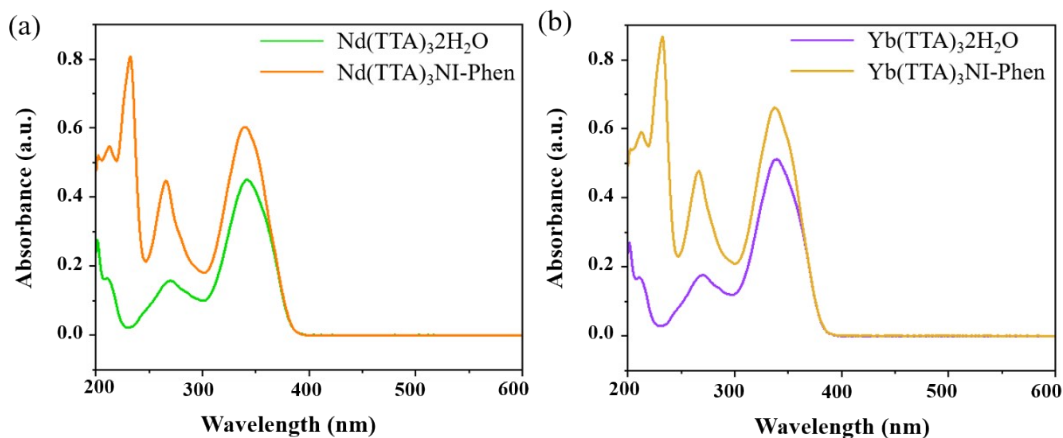


Figure S11. UV-vis spectra of $\text{Ln}(\text{TTA})_32\text{H}_2\text{O}$ and $\text{Ln}(\text{TTA})_3\text{NI-Phen}$ in anhydrous ethanol

(1×10^{-5} mol/L) at room temperature. (a): Nd(TTA)₃2H₂O and Nd(TTA)₃NI-Phen, (b):

Yb(TTA)₃2H₂O and Yb(TTA)₃NI-Phen.

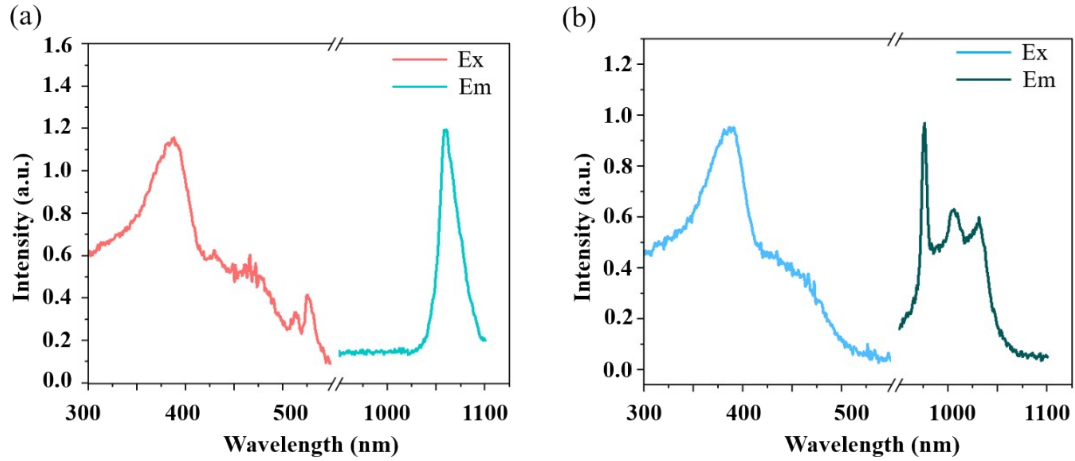


Figure S12. Fluorescence spectroscopy of Ln(TTA)₃NI-Phen powder at room temperature. (a): Nd(TTA)₃NI-Phen ($\lambda_{\text{ex}}=388$ nm, $\lambda_{\text{em}}=1058$ nm). (b): Yb(TTA)₃NI-Phen ($\lambda_{\text{ex}}=386$ nm, $\lambda_{\text{em}}=976$ nm).

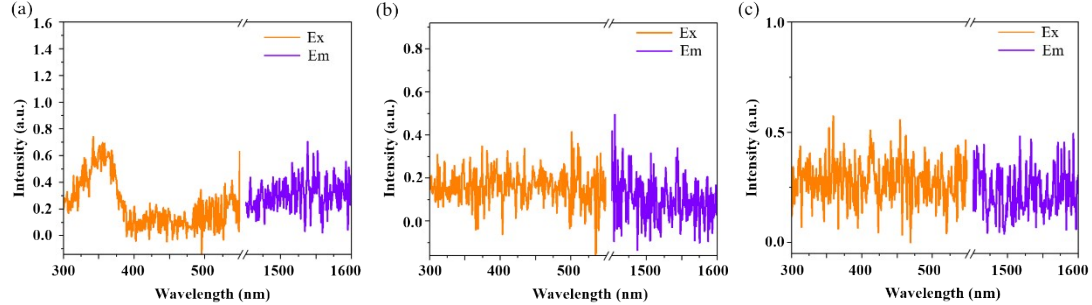


Figure S13. Fluorescence spectroscopy of Er(TTA)₃NI-Phen (1×10^{-5} mol/L) in DMSO (a), RPMI1640 (b) and DMEM (c) at room temperature.

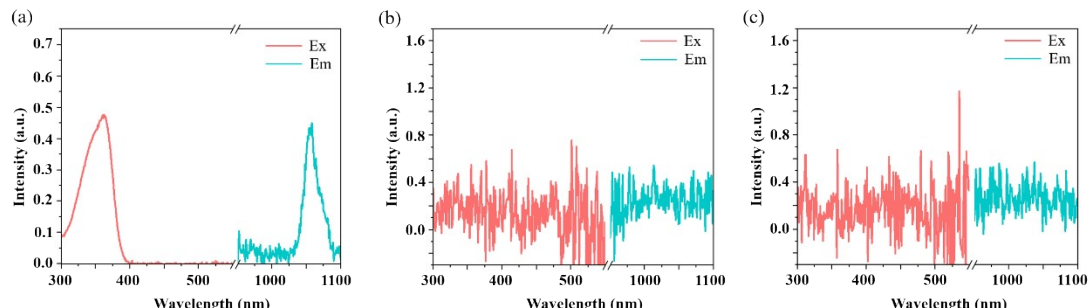


Figure S14. Fluorescence spectroscopy of Nd(TTA)₃NI-Phen (1×10^{-5} mol/L) in DMSO (a),

RPMI1640 (b) and DMEM (c) at room temperature ($\lambda_{\text{ex}}=362 \text{ nm}$, $\lambda_{\text{em}}=1058 \text{ nm}$).

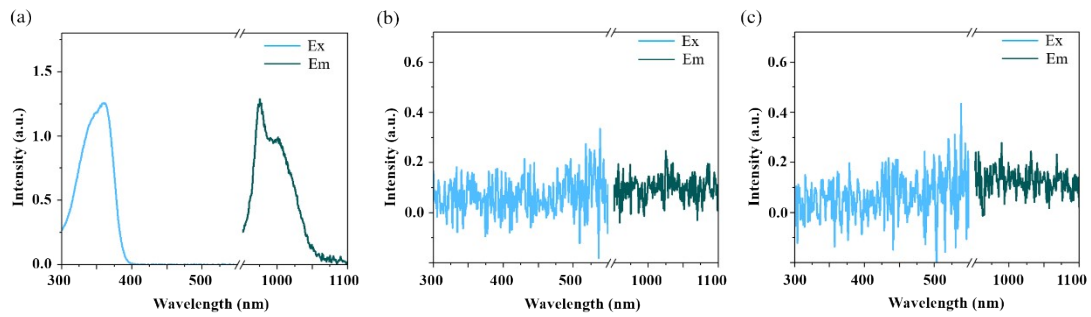


Figure S15. Fluorescence spectroscopy of $\text{Yb}(\text{TTA})_3\text{NI-Phen}$ ($1 \times 10^{-5} \text{ mol/L}$) in DMSO (a),

RPMI1640 (b) and DMEM (c) at room temperature ($\lambda_{\text{ex}}=360 \text{ nm}$, $\lambda_{\text{em}}=976 \text{ nm}$).

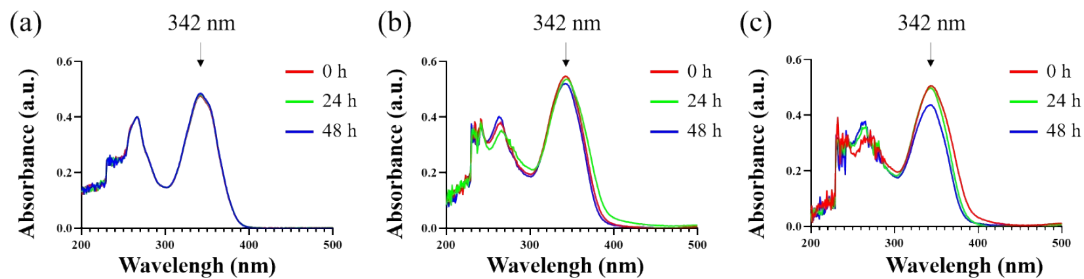


Figure S16. UV-vis spectra of $\text{Er}(\text{TTA})_3\text{NI-Phen}$ ($1 \times 10^{-5} \text{ mol/L}$) in DMSO (a), RPMI1640 (b)

and DMEM (c) at various time intervals (0-48 hours).

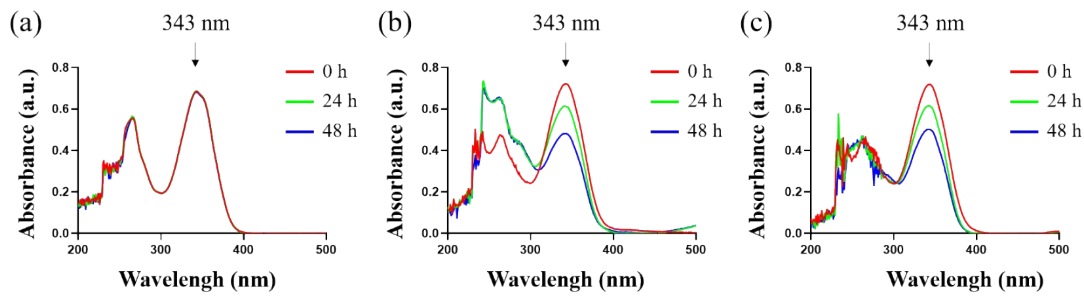


Figure S17. UV-vis spectra of $\text{Nd}(\text{TTA})_3\text{NI-Phen}$ ($1 \times 10^{-5} \text{ mol/L}$) in DMSO (a), RPMI1640 (b)

and DMEM (c) at various time intervals (0-48 hours).

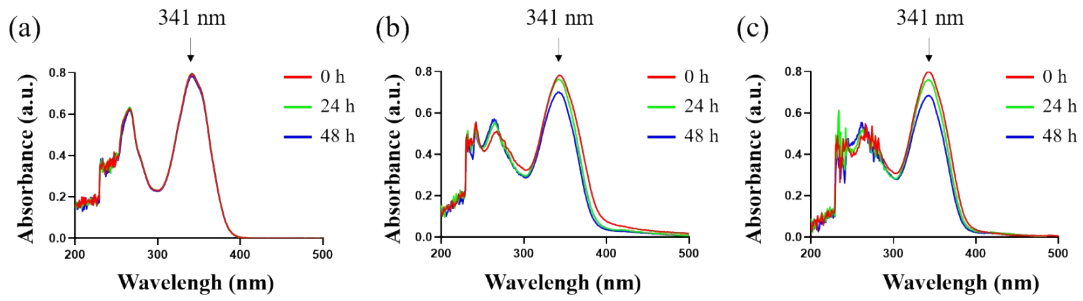


Figure S18. UV-vis spectra of Yb(TTA)₃Ni-Phen (1×10⁻⁵ mol/L) in DMSO (a), RPMI1640 (b)

and DMEM (c) at various time intervals (0-48 hours).

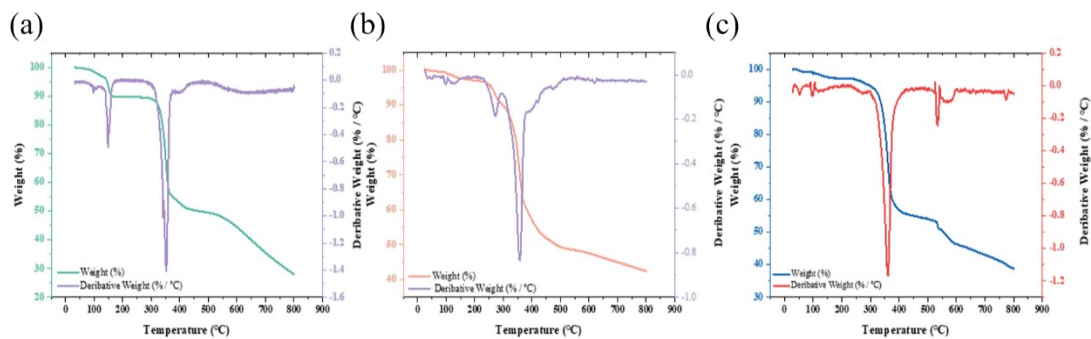


Figure S19. TGA curves of Er(TTA)₃Ni-Phen (a), Nd(TTA)₃Ni-Phen (b) and Yb(TTA)₃Ni-Phen

(c) in nitrogen.

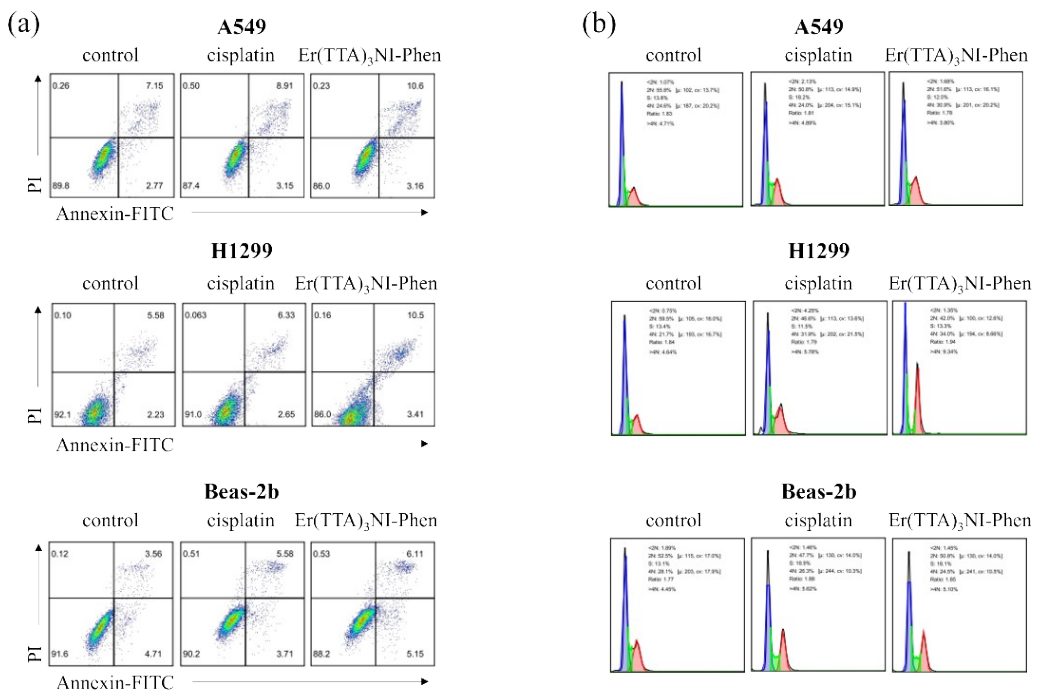


Figure S20. Cells apoptosis (a) and cells cycle (b) induced by cisplatin (5 μM) and Er(TTA)₃Ni-

Phen (1 μ M). control group: equal volume DMSO.

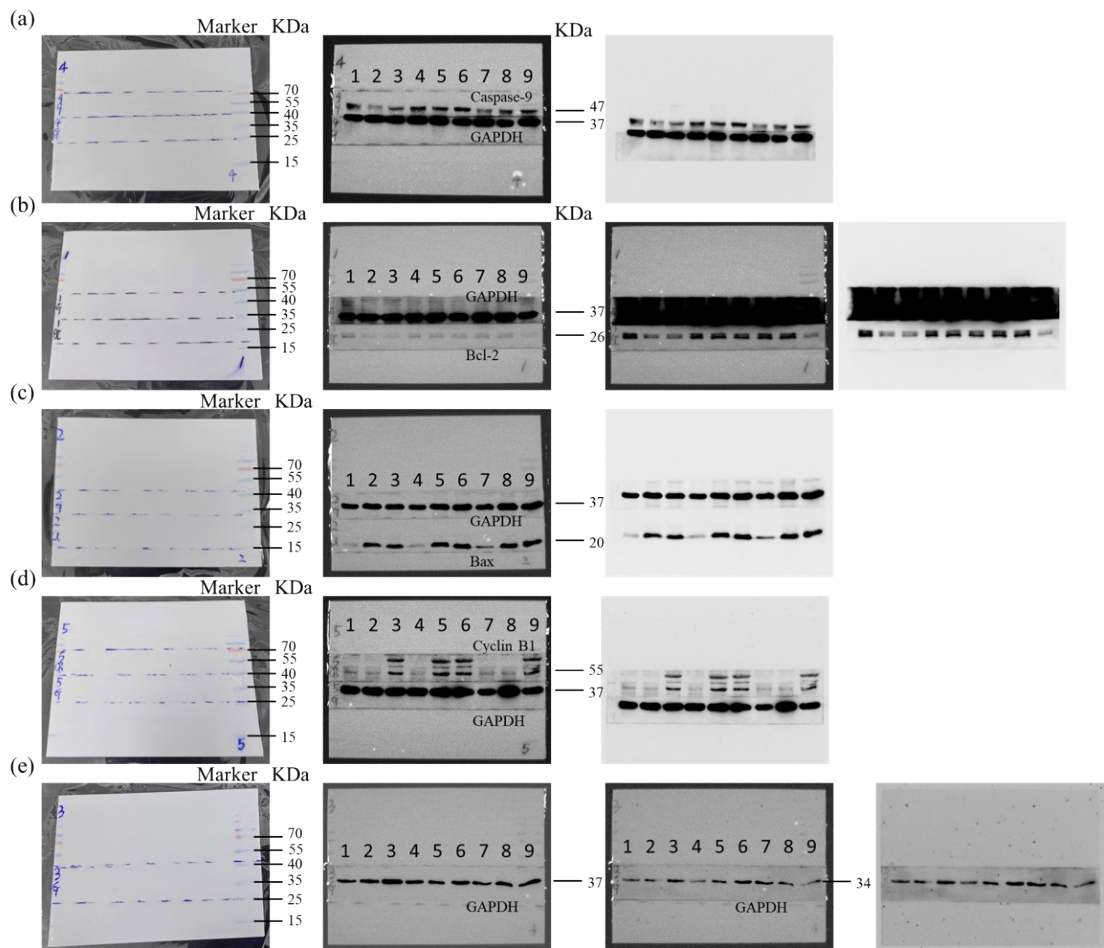


Figure S21. Raw data associated with the WB data provided in Fig. 8 (d). (a): Caspase-9 protein. (b): Bcl-2 protein. (c): Bax protein. (d): Cyclin B1 protein. (e): *p*-CDK1 protein. The *p*-CDK1 protein and GAPDH protein are very similar in size, and markers cannot accurately separate the two proteins. So first, stain the GAPDH protein imprint with GAPDH antibody, then wash it off with eluent, and re-incubate *p*-CDK1 antibody on the same band to stain *p*-CDK1 protein. Lane 1, 2, 3: A549 cells treated with DMSO, cisplatin, Er(TTA)₃NI-Phen. Lane 4, 5, 6: H1299 cells treated with DMSO, cisplatin, Er(TTA)₃NI-Phen. Lane 7, 8, 9: Beas-2b cells treated with DMSO, cisplatin, Er(TTA)₃NI-Phen.

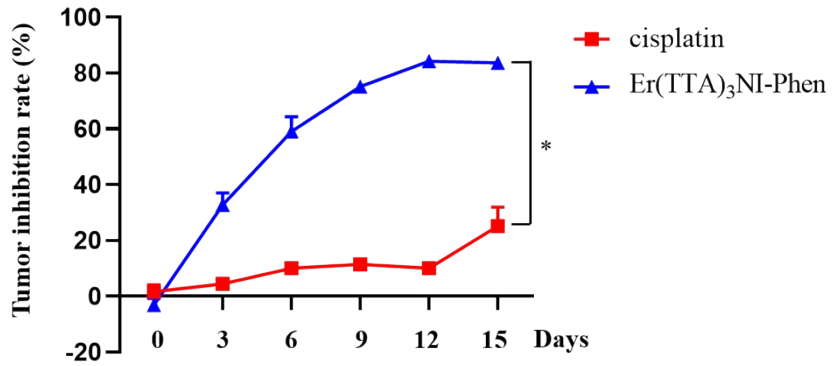


Figure S22. Tumor inhibition rates of mice injected with cisplatin and $\text{Er}(\text{HTTA})_3\text{NI-Phen}$. Value graphed as means \pm SD ($n=5$). $^*P<0.05$ vs cisplatin.

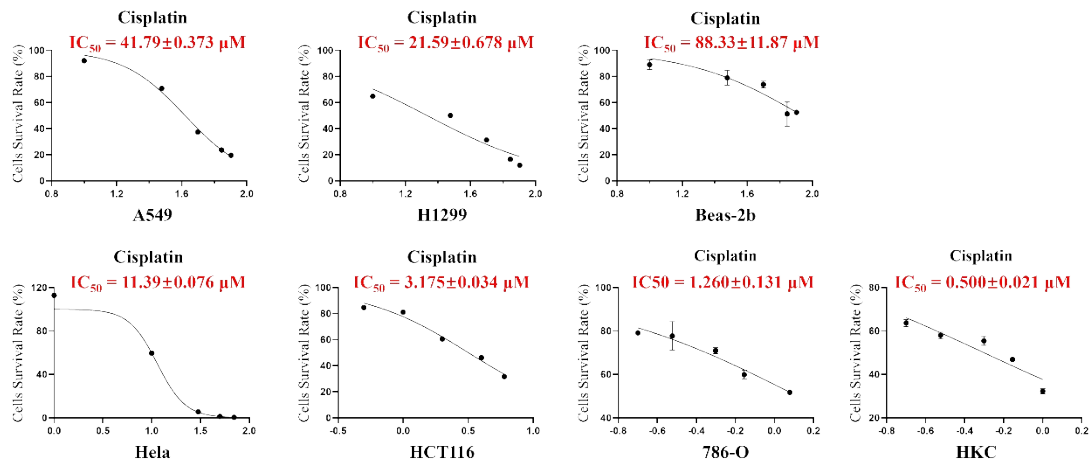


Figure S23. The curve fits of dose survival curves on cisplatin against seven cells.

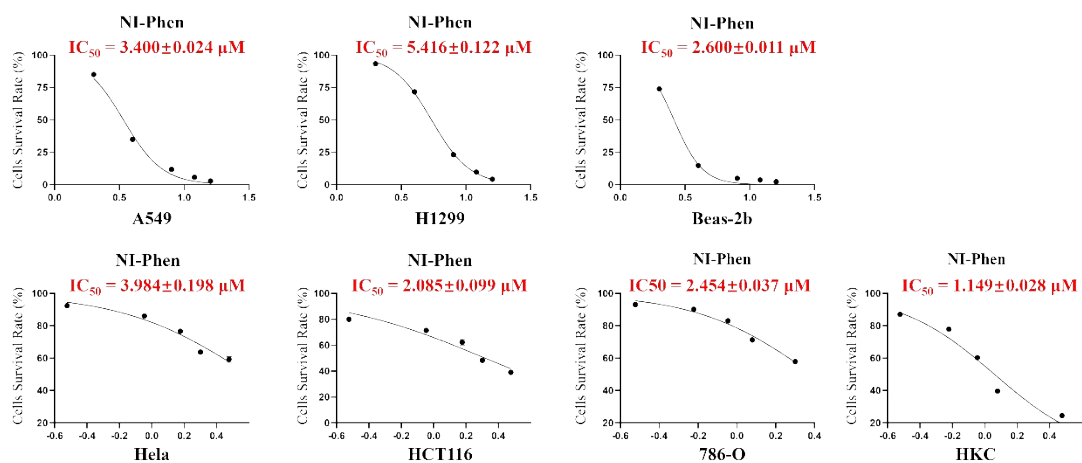


Figure S24. The curve fits of dose survival curves on NI-Phen against seven cells.

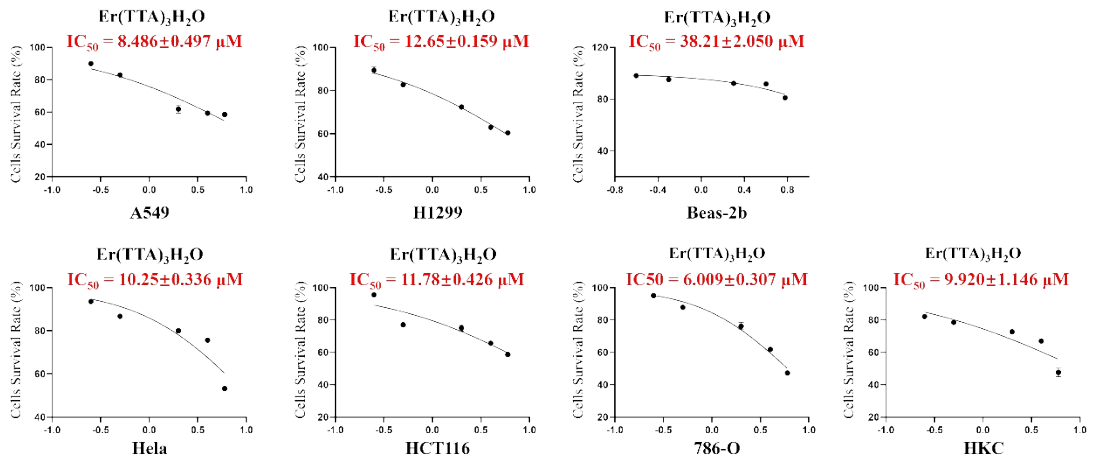


Figure S25. The curve fits of dose survival curves on $\text{Er}(\text{TTA})_3\text{H}_2\text{O}$ against seven cells.

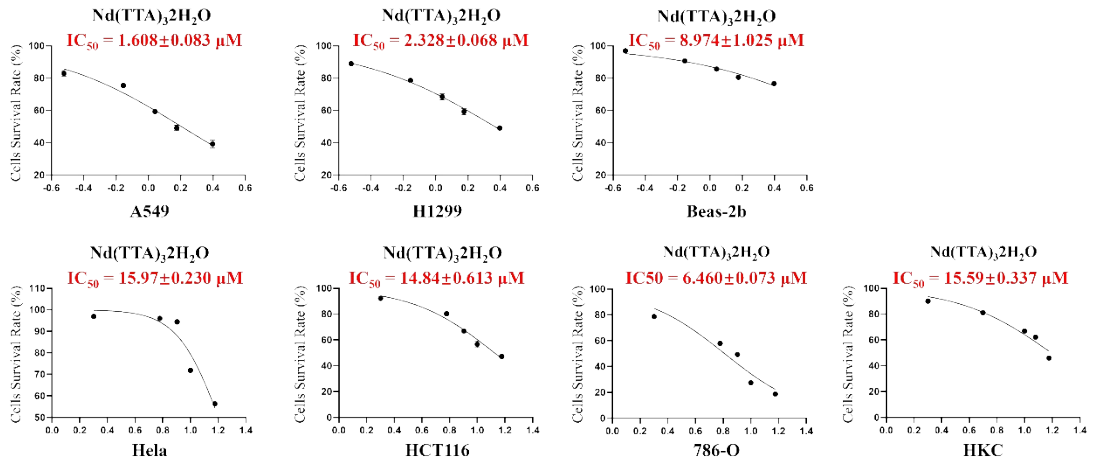


Figure S26. The curve fits of dose survival curves on $\text{Nd}(\text{TTA})_32\text{H}_2\text{O}$ against seven cells.

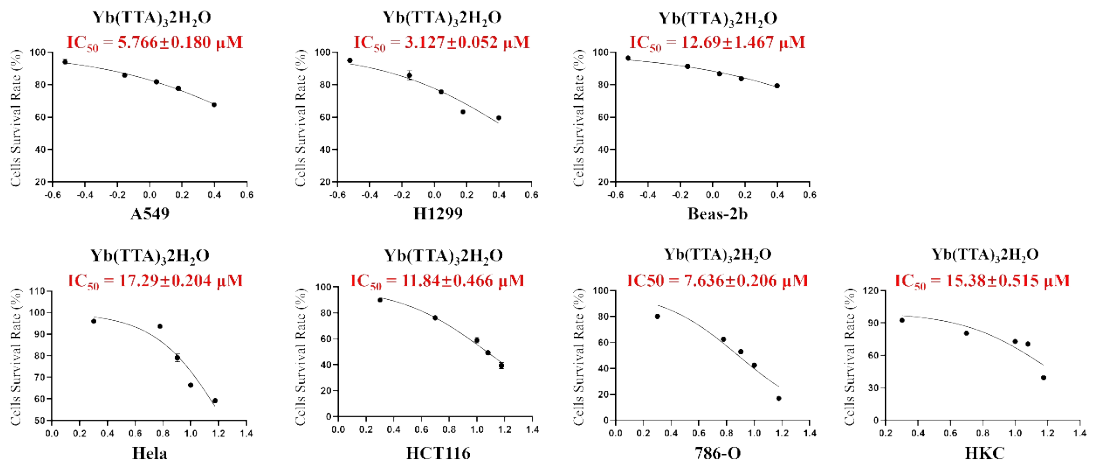


Figure S27. The curve fits of dose survival curves on $\text{Yb}(\text{TTA})_32\text{H}_2\text{O}$ against seven cells.

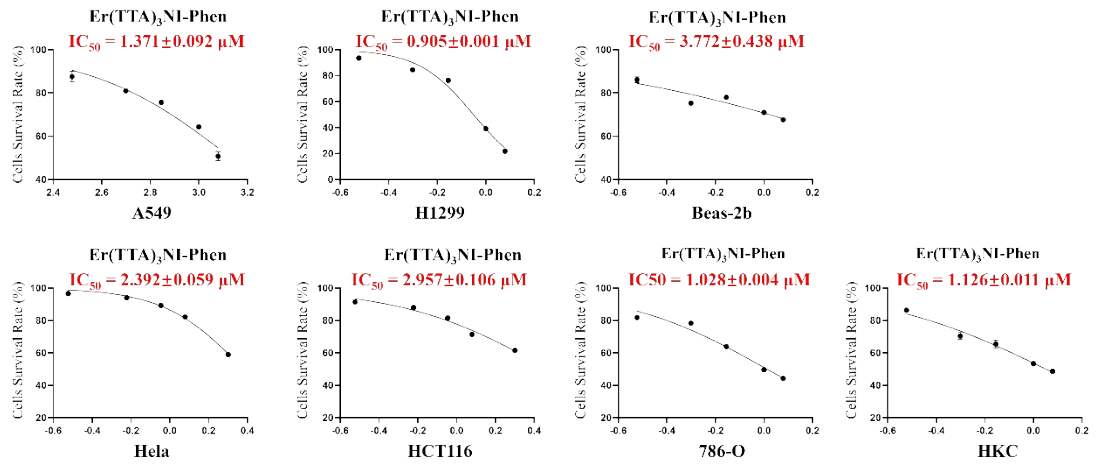


Figure S28. The curve fits of dose survival curves on $\text{Er}(\text{TTA})_3\text{Ni-Phen}$ against seven cells.

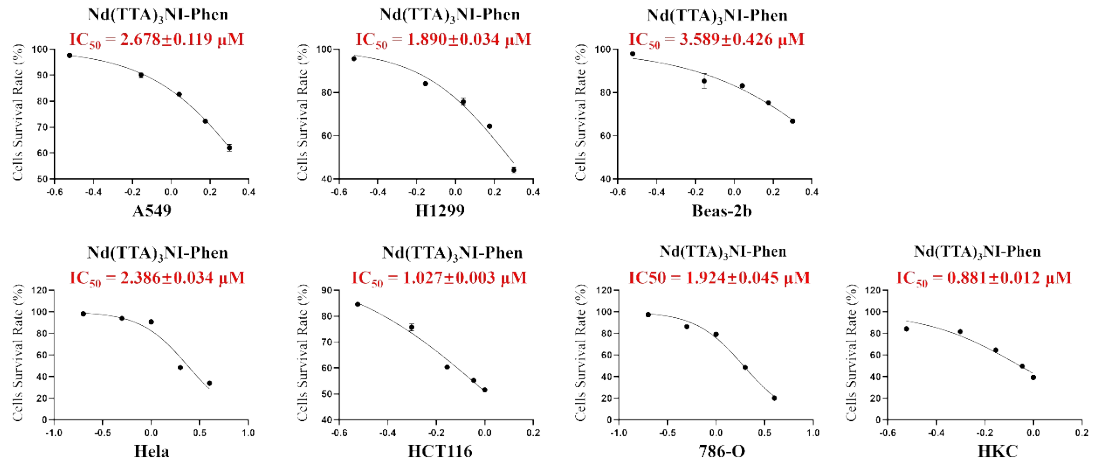


Figure S29. The curve fits of dose survival curves on $\text{Nd}(\text{TTA})_3\text{Ni-Phen}$ against seven cells.

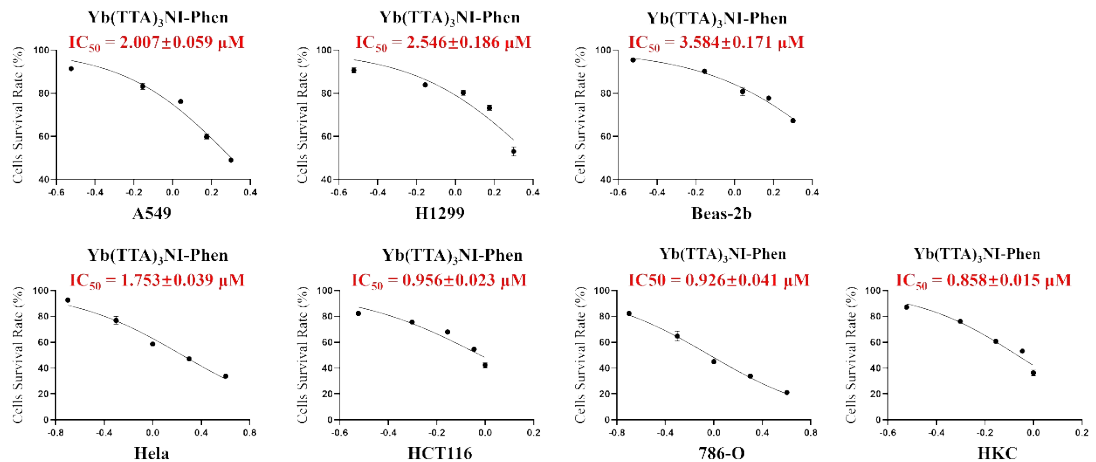


Figure S30. The curve fits of dose survival curves on $\text{Yb}(\text{TTA})_3\text{Ni-Phen}$ against seven cells.

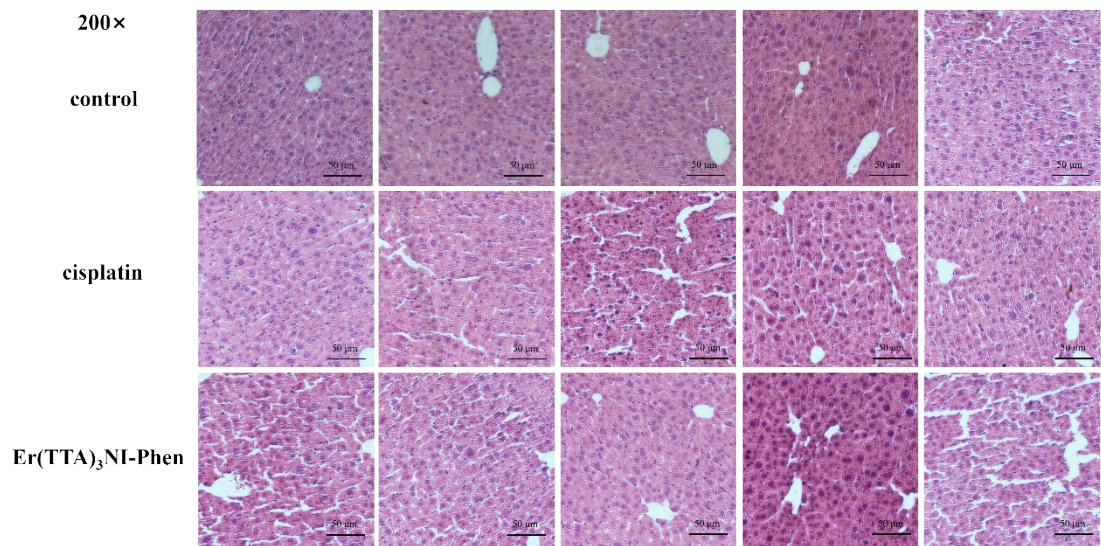


Figure S31. HE staining images of liver tissues from each group. The magnification is 200 times,

and each group consists of liver tissue from 5 mice.

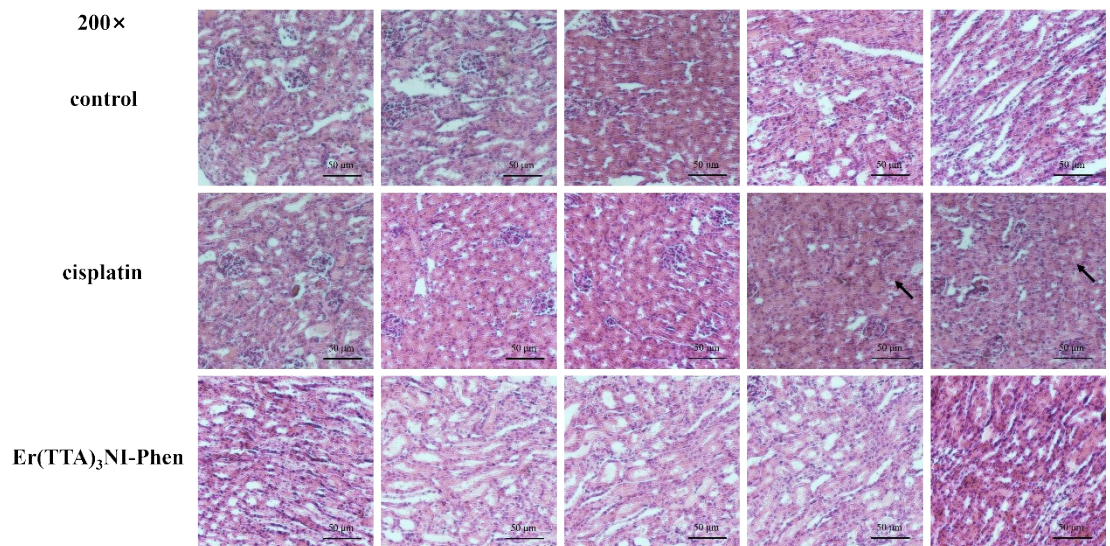


Figure S32. HE staining images of kidney tissues in each group. The magnification is 200 times,

and each group consists of kidney tissue from 5 mice. The black arrow marked the disappearance

of normal glomerular structure and renal interstitial edema.

Table S1. The 95% Confidence Interval of Hill Slope and IC₅₀ value in Table 1.

Groups	95% CI ^a	A549	H1299	Beas-2b
cisplatin	Hill Slope -3.103 to -1.642	-3.103 to -1.642	-2.285 to -0.429	-3.161 to -0.408

	IC ₅₀	36.40 to 46.99	7.349 to 36.21	62.32 to 304.3
	Hill Slope	-4.878 to -1.922	-3.256 to -2.636	-5.823 to -2.710
NI-Phen	IC ₅₀	2.909 to 3.975	5.172 to 5.669	2.332 to 2.910
	Hill Slope	-0.944 to -0.234	-0.631 to -0.403	-6.433 to -0.094
Er(TTA) ₃ H ₂ O	IC ₅₀	4.180 to 67.92	8.994 to 20.80	7.416 to infinity
	Hill Slope	-1.554 to -0.686	-1.211 to -0.859	-1.315 to -0.520
Nd(TTA) ₃ 2H ₂ O	IC ₅₀	1.288 to 2.174	2.066 to 2.702	4.981 to 32.80
	Hill Slope	-1.057 to -0.752	-1.839 to -0.529	-1.072 to -0.567
Yb(TTA) ₃ 2H ₂ O	IC ₅₀	4.661 to 7.648	2.145 to 8.796	7.390 to 31.50
	Hill Slope	-2.471 to -0.797	-6.579 to -2.248	-1.233 to -0.191
Er(TTA) ₃ NI-Phen	IC ₅₀	1.093 to 2.268	0.786 to 1.003	1.803 to 246.1
	Hill Slope	-1.884 to -1.529	-3.034 to -1.178	-2.013 to -0.735
Nd(TTA) ₃ NI-Phen	IC ₅₀	2.510 to 2.869	1.631 to 2.452	2.529 to 7.471
	Hill Slope	-2.497 to -0.930	-3.951 to -0.367	-1.828 to -0.900
Yb(TTA) ₃ NI-Phen	IC ₅₀	1.671 to 2.855	1.757 to 22.52	2.763 to 5.645

^a The 95% Confidence Interval (95% CI) represents a 95% confidence level that the interval contains the true range of Hill Slope and IC₅₀ value.

Table S2. The 95% Confidence Interval of Hill Slope and IC₅₀ value in Table 2.

Groups	95% CI ^a	HeLa	HCT116	786-O	HKC
cisplatin	Hill Slope	-infinity to -1.303	-1.458 to -0.769	-1.111 to -0.491	-1.295 to -0.216
	IC ₅₀	7.535 to 16.75	2.545 to 4.079	0.974 to 2.351	0.301 to 0.933

	Hill Slope	-1.833 to -0.590	-1.662 to -0.406	-2.041 to -0.974	-3.087 to -0.749
NI-Phen	IC ₅₀	2.869 to 8.813	1.459 to 4.055	1.990 to 3.596	0.834 to 1.760
	Hill Slope	-3.882 to -0.142	-1.315 to -0.125	-1.504 to -0.610	-1.283 to -0.041
Er(TTA) ₃ H ₂ O	IC ₅₀	4.760 to 9404	4.783 to 7444	4.550 to 9.669	3.421 to infinity
	Hill Slope	-6.088 to -1.036	-2.229 to -0.880	-3.898 to -0.590	-2.668 to -0.615
Nd(TTA) ₃ 2H ₂ O	IC ₅₀	12.90 to 34.59	11.07 to 18.40	3.809 to 9.171	12.08 to 29.29
	Hill Slope	-3.551 to -0.591	-1.875 to -0.987	-4.172 to -0.531	-12.35 to -0.049
Yb(TTA) ₃ 2H ₂ O	IC ₅₀	12.77 to 64.54	10.35 to 13.86	4.620 to 11.41	9.721 to infinity
	Hill Slope	-2.679 to -1.669	-1.621 to -0.764	-2.126 to -0.920	-1.640 to -0.912
Er(TTA) ₃ NI-Phen	IC ₅₀	2.154 to 2.783	2.252 to 4.960	0.876 to 1.320	0.981 to 1.377
	Hill Slope	-3.970 to -0.810	-1.874 to -1.017	-2.505 to -1.260	-4.302 to -1.035
Nd(TTA) ₃ NI-Phen	IC ₅₀	1.616 to 4.241	0.911 to 1.236	1.606 to 2.318	0.745 to 1.193
	Hill Slope	-1.284 to -0.662	-3.329 to -0.638	-1.138 to 0.774	-3.538 to -1.100
Yb(TTA) ₃ NI-Phen	IC ₅₀	1.331 to 2.429	0.768 to 1.731	0.783 to 1.093	0.731 to 1.098